O.E.C.D. HIGH TEMPERATURE REACTOR PROJECT

Conf-690627--3

DRAGON

Dragon Project Report

HIGH TEMPERATURE RADIATION INDUCED CREEP IN GRAPHITE

by

R. BLACKSTONE*
L.W. GRAHAM**
M.R. EVERETT**

PAPER PRESENTED AT THE 9th CARBON CONFERENCE. BOSTON. U.S.A. JUNE 1969

A.E.E. Winfrith, Dorchester, Dorset, England

OCTOBER, 1969

DISCLAIMER

HIGH TEMPERATURE RADIATION INDUCED CREEP IN GRAPHITE

by

R. BLACKSTONE*

L. W. GRAHAM**

M. R. EVERETT**

ABSTRACT

The irradiation creep of graphite has been determined at 600, 800, 900 and 1200°C by successive irradiations in the High Flux Reactor Petten, of specially designed assemblies in which two or more graphites having differing shrinkage rates are used in opposition to provide tensile or compressive stress in a specimen. The experimental technique is described and the results are compared with the predicted calculated behaviour of the assemblies.

Tensile Creep strain in excess of 2% have been obtained. Attempts are made to correlate the observed creep constants with other physical properties.

---

*Reactor Centrum Nederland, Petten, The Netherlands.

**O.E.C.D. Dragon Project, Winfrith, Dorset, England.

CONTENTS

LIST OF TABLES

LIST OF FIGURES

HIGH TEMPERATURE RADIATION INDUCED CREEP IN GRAPHITE

by

R. BLACKSTONE
L.W. GRAHAM
M.R. EVERETT

1. INTRODUCTION

The existence of irradiation induced plasticity in graphite subjected to stress has been a significant factor in the development of gas cooled reactors. Stress levels in graphite components subjected to differential effects arising from flux and temperature gradients are minimized by irradiation creep, giving the designer more freedom than is normally possible with brittle materials. The phenomenon is particularly important in the design of high temperature gas cooled reactors as the fission product retaining fuel, in the form of coated particles, is contained in graphite which has to carry heat fluxes which may be as high as 50 W/cm^2. Without significant irradiation induced plasticity the effects arising from the combination of thermal stress and stresses induced by differential irradiation shrinkage might seriously limit the potential of such reactors.

Since 1961 the O.E.C.D. Dragon Project has been engaged on a programme of graphite irradiations at temperatures in the range 600 - 1200°C in the High Flux Reactor at Petten, The Netherlands. An important part of this work has been the investigation of irradiation creep. Apart from a desire to understand the mechanism of the creep process the work was undertaken to provide technical data on:

(i) the steady state irradiation creep coefficient (strain per unit stress per unit dose) and its temperature dependence,

(ii) the maximum creep strain to failure.

In this paper the experimental methods and some of the results obtained are described.

2. PRINCIPLE OF THE METHOD USED

Ideally a creep experiment should be performed under controlled stress. This either involves the use of a dead weight [1] or a suitable pneumatic or

hydraulic mechanism, [2] [3], and a continuous recording of strain. There are some practical disadvantages in performing these experiments under irradiation, the most important being that it requires much space. From the practical point of view a much simpler solution, requiring far less irradiation space, is to study the creep under conditions of approximately constant strain rate, making use of the difference in shrinkage or expansion rates of different graphites or of the same graphite in different directions. The idea goes back to Losty [4] and has since been applied by several investigators [5], [6], and [7] and has been used in the present work.

Figs. 1 and 2 show the tensile creep assembly. The specimen has the shape of a tensile test specimen called "the dumb-bell", with its neck surrounded by a (split) sleeve. The sleeve is chosen so that under irradiation it shrinks less rapidly than the dumb-bell or even expands. From the moment that the length of the sleeve and the neck of the dumb-bell are just equal the sleeve will restrain the shrinkage of the dumb-bell, which will accordingly become stressed in tension while the split sleeve becomes stressed in compression.

When the difference in rates of dimensional change between the dumb-bell and split sleeve material is small, one can increase the strain in the specimen roughly n-fold by concentrating the elongation in 1/n-th part of the dumb-bell length, which is given a much smaller cross-section than the sleeve and the rest of the dumb-bell. In practice the ratio of the cross sections cannot be made smaller than 1:9.

An experiment in compression is also possible. Fig. 3 shows the compressive assembly. Here the specimen, surrounded by a spacer which also serves as a control giving the free shinkage, is placed inside a rapidly shrinking outer restrainer, so that in effect the space available for the specimen shrinks more rapidly than the specimen itself. From the moment that the specimen fits exactly in the available space it will be loaded in compression, the strain rate being determined by differences in shrinkage rates, lengths, cross sections and creep coefficients of the components.

The results are analysed on the basis of the assumption that the steady state creep strain is linearly proportional to stress σ and integrated neutron flux ϕt.

$$\varepsilon_{II} = k\sigma\phi t = k\sigma N \qquad (1)$$

Evidence that this assumption is correct to a first approximation at the flux levels which occur in the present experiment can be found in the work of Kennedy [3].

In a constant stress experiment the diagram of strain versus neutron dose resembles the diagram of strain versus time in a normal thermal creep experiment. After a rapid initial straining the creep strain becomes a linear function of the neutron dose ϕt. The first part of the process is called the transient creep, the linear part is called the steady-state creep. From the relation of the zero dose intercept and the stress it is found that the transient creep strain, ε_I, almost equals the elastic strain of the irradiated graphite under the same stress. In fact $\varepsilon_I \tilde{=} 0.95\ \sigma/E$, where σ is the stress and E is the Young's Modulus of the irradiated graphite. For the present purpose it appears that the transient creep process is represented with sufficient accuracy by the relation:

$$\varepsilon_I = \frac{\sigma}{E}\,(1 - e^{-aN}) \qquad (2)$$

where $N = \phi t$ is the neutron dose in units 10^{20} n.cm^{-2} and a is a "time constant" which seems to be of the order 1 . $(10^{20}\ \text{n.cm}^{-2})^{-1}$. A plot of the logarithm of the stress versus the logarithm of the strain rate yields an approximately straight line with a slope equal 1. This is the basis for relation (1), which defines the steady state radiation creep constant k.

Starting from this relation it is possible to find expressions representing the stress build-up in the various parts of the assembly. These expressions are developed in Appendix I.

As expected the stress depends on the rate of unrestrained dimensional change of the specimen and the restrainer and their radiation creep constants. In general the rates of dimensional change are not constant but they vary with neutron fluence.

In the present series of experiments in the relevant range of neutron fluences it was found that the free dimensional changes of both material of the specimen and that of the restrainer could in most cases be represented by some parabolic function of the neutron fluence and only in a few cases they were linear functions of the neutron fluence.

Neglecting the primary creep for the moment, it can be shown that the stress in a given component as a function of the neutron fluence is given by

$$\sigma(N) = \left(\frac{R_2}{Q} - \frac{2R_1}{Q^2}\right) \cdot (1-e^{-QN}) + \frac{2R_1}{Q}\,N \qquad (3)$$

where:

$\sigma(N)$ is the stress after an effective fast neutron fluence N

N is the effective fast neutron fluence, i.e. the fluence counted from the moment that restraint occurs.

R_1 and R_2 are effective stressing rates, having the dimension stress per (unit fluence)^2 and stress per unit fluence respectively. If the dimensional changes of the specimen (A) and the restrainer (C) can be represented by

$$\frac{\Delta L}{L_o}(A) = a_1 D^2 + a_2 D + a_3 \quad \text{and} \quad \frac{\Delta L}{L_o}(C) = c_1 D^2 + c_2 D + c_3 \qquad (4)$$

where D is the total fast neutron fluence, then R_1 is proportional to $-(a_1 - c_1)E_A$ and R_2 to $-(a_2 - c_2)E_A$ where E_A is the Young's Modulus of the specimen. R_1 and R_2 further depend on the lengths of the various parts of the assembly, the ratio of their cross-sections and the ratio of their Young's Moduli.

Q is an effective creep strain rate of the assembly. $Q = K^+ . E_A$, the Young's Modulus of the specimen multiplied by a weighted average irradiation creep constant for the assembly as a whole. In practice Q is of the order $0.3 - 2.0\ (10^{20} \text{ncm}^{-2})^{-1}$.

For values of N sufficiently large to make $1 - e^{-QN} \cong 1$, the stress is seen to increase linearly with the neutron fluence N.

The expression is simplified when the dimensional changes of both the specimen and the restrainer are linear functions of the neutron fluence. In that case $R_1 = o$ and a constant equilibrium stress

$$\sigma(N) = \sigma_e = \frac{R_2}{Q} \quad \text{is established.} \qquad (5)$$

By proper selection of the materials and the dimensions one can give an assembly any desired R-values within certain limits. Both R_1, R_2 and Q are specific for an individual assembly.

Strictly speaking R_1, R_2 and Q are not constant since the Young's Modulus changes upon irradiation. As at least in unrestrained specimens however the Young's Modulus shows a steep increase in the first stage of the irradiation and after that only shows relatively minor changes, up to a fluence of $\sim 25 \times 10^{20}$ n.cm^{-2}, [8], R_1, R_2 and Q are treated as constants as a first approximation for the present purpose. The Young's Modulus value of the irradiated graphite is used.

If one takes into account the primary creep process the formula representing the stress build-up becomes much more complicated. One might say that

every increment of stress gives rise to an increment of transient creep strain which has the effect of partly relaxing the stress. In the case where a constant stress is established only the rate of build-up of this stress is modified by the presence of the transient creep. But if the stress increases with neutron fluence one must assume that the transient creep process keeps playing a role over the entire fluence range. It was found that for the neutron fluence range where $1-e^{-QN}=1$, $\sigma(N)$ <u>with</u> transient creep can be approximated with good accuracy by

$$\sigma(N) = \frac{1}{Q}\left(R_2 + 2R_1N - 4\frac{R_1}{Q}\right) \qquad (6)$$

On the basis of the foregoing it appears that the irradiation creep constant of a material can be found from a restrained shrinkage experiment if the following data are known:

1. The stress
2. The unrestrained dimensional changes
3. The restrained dimensional changes
4. The dimensions of the different parts of the assembly, both lengths and cross-sections
5. The Young's Modulus of all the parts
6. The thermal expansion coefficient of all the parts
7. The irradiation conditions, time, neutron flux density and the irradiation temperature.

Suppose that one is able to choose the dimensions of the specimen and the restrainer so that the restraint starts exactly at the beginning of the irradiation. After a neutron fluence N_1, sufficiently large to make $1-e^{-aN_1} \cong 1$, the stress in the specimen A is σ_A. One can then find Q by solving equation (6).

$$Q = \frac{R_2 + 2R_1N_1 + \sqrt{(R_2 + 2R_1N_1)^2 - 16R_1\sigma_A}}{2\sigma_A} = k^+ \cdot E_A \qquad (7)$$

where k^+ in the effective radiation creep constant for the assembly as a whole. In fact N_1 is the neutron fluence during which the restraint occurred. In general N_1 need not be identical to the total neutron fluence D. It is therefore necessary either to design the assembly so that the specimen and the restrainer make contact at the beginning of the experiment at the irradiation temperature, or else to measure the gap between the specimen and the restrainer and to calculate the neutron fluence needed to close this gap.

It is possible to find k_A and k_C separately from k^+ since specimen and restrainer stress each other mutually. Accordingly the stress in the restrainer C is related to that in the specimen A as follows $\sigma_c = -\frac{O_A}{O_C} \cdot \sigma_A$ where O_A and O_C are the cross-sectional areas of the specimen and the restrainer. The steady state creep strain is

$$\varepsilon_{II}(N) = k \int_0^N \sigma\,(N)\, dN \qquad (8)$$

and thus

$$\frac{\varepsilon_{II}(N)_C}{\varepsilon_{II}(N)_A} = -\frac{O_A\, k_C}{O_C\, k_A} \qquad (9)$$

Both $\varepsilon_{II}(N)_C$ and $\varepsilon_{II}(N)_A$, the steady state creep strains in the two components, can be determined experimentally as

$$\varepsilon_{II} = \varepsilon_{total} - \varepsilon_I - \varepsilon_T \qquad (10)$$

where ε_{total} is the apparent creep strain, equal to the difference of restrained and unrestrained dimensional change

ε_I is the primary creep strain $= \frac{\sigma}{E}$

ε_T is the strain due to change in thermal expansion coefficient, $\Delta\alpha$

$\varepsilon_T = (T_{irr} - T_m)\Delta\alpha$

T_{irr} is the irradiation temperature

T_m is the temperature at which dimensional measurements are performed.

The relationship between k^+ and k_A and k_C is given in the Appendix.

If, after an initial irradiation for N_1 n.cm^{-2} where $1-e^{-QN_1} \simeq 1$, one can reirradiate the same assembly under the same circumstances for another period in which it receives an additional neutron fluence ΔN, in which the steady state creep strain of a component changes from ε_1 to ε_2, and in which the stress increases from σ_1 to σ_2, then the creep constant k of that component can also be obtained as

$$k = \frac{\varepsilon_2 - \varepsilon_1}{\frac{\sigma_2 + \sigma_1}{2} \cdot \Delta N} \qquad (11)$$

The implicit assumption in every case is that it is possible to interrupt the experiment and that cooling down and reheating, for instance between two reactor cycles, causes no large irreversible structural changes in the materials.

The following points were checked to see whether the results were internally consistent and whether they were consistent, within the experimental accuracy, with the theory outlined above.

a) For double necked dumb-bells in the present experiments the ratio of the cross-sections of the thin and thick neck is about 0.33, so that the creep strains of the thick neck must be 0.33 x that of the thin neck. This could be used to check whether the dimensional changes found in control specimens were representative of the free dimensional changes of the dumb-bell material.

b) As explained above the creep constant of the whole assembly k^+, and from this the creep constant of the components separately, k_A and k_C, are obtained from the unrestrained dimensional changes of the components, the measured stress, and the ratio of the steady state creep strains in the components. The actual values of the steady state creep strains are not used to obtain the creep constants. Once the creep constants are known however one can calculate the creep strains by taking the integral of the stress as function of the neutron fluence, multiplied by the creep constant, and compare this with the values obtained by measurement. A computer programme is available to calculate (formulae 7 and 15 of the Appendix) the stress build-up and the restrained dimensional changes for any assembly when the free dimensional changes, the Young's Moduli and the creep constants are given.

3. EXPERIMENTAL METHODS

The stress present in the specimen at the end of the irradiation is relieved, upon cooling down, partly or totally, depending on the difference in thermal expansion coefficient of the specimen and the restrainers. On reheating the assembly to the irradiation temperature in a laboratory furnace the stress reappears. The stress can be measured reproducibly in several runs. This does not in fact prove that the cooling down and unloading of the specimen and the restrainers after irradiation or even between the various cycles of the irradiation does not give rise to irreversible structural changes in the materials. It has been assumed that such changes do not occur.

The stress is measured in two steps. For the tensile assembly the procedure is as follows. First the elastic strain is obtained by measuring

with a suitable dilatometer the length at the irradiation temperature of the assembly as it was irradiated, and afterwards that of the dumb-bell alone, without restrainer (split sleeve). The difference of these two lengths gives the total elastic elongation of the dumb-bell at the irradiation temperature, from which the elastic strain in both the thin and thick neck can be calculated. Also one obtains the thermal expansion coefficient of the restrained dumb-bell, assuming that the thermal expansion of the dumb-bell shoulders is not too different from that of the part of the dumb-bell restrainedin tension. The thermal expansion of the restrainers can either be measured directly or they can be calculated from that of the assembly if one knows the Young's Moduli of the various components and the gap at room temperature.

Then the force necessary to produce the measured elastic elongation is measured with a tensile test, for the sake of simplicity at room temperature. From sonic measurements at elevated temperatures the temperature coefficient of Young's Modulus is known. This temperature correction is of the order of $+\sim 10\%$.

For the compressive assembly the method is similar. With the dilatometer one measures the length of the specimen, the inner restrainer, and the end plug by bringing the push rod of the dilatometer in contact with the inner restrainer through a narrow hole in the bottom of the outer restrainer. For the second run the restraint can be effectively removed by loosening the threaded plug by one turn. In this way one measures the total elastic compression of the inner restrainer, plug and specimen and the individual elastic strains can then be found if the Young's Modulus and the cross-sections of these three parts are known. In this way the elastic stress in the specimen and the inner restrainer is found. The Young's Modulus of the specimens and the inner restrainer are measured with a sonic method, that of the plug is estimated.

For the strain measurement a simple fused silica dilatometer is used, operating in vacuo, in which the length changes are measured with a Daytronic Linear Displacement Transducer. (Fig. 4 gives a schematic drawing of the dilatometer.)

For the tensile test a small tensile testing machine was designed and built. Its main features, shown diagrammaticaly in Figs. 5 and 6, are:

(a) The specimen (A) is mounted in gimbals (B) to minimize bending moments.

(b) Slides with ball bearings (C) are used for the moving part to minimize friction.

(c) For the same reason the load is transmitted to the carriage (D)

by a rubber membrane (E), closing the open end of a brass cylinder (F) which can be pressurised with air to about 2 atm.
By means of a needle valve the pressure can be regulated continuously. The pressure in the cylinder is measured with a calibrated Daytronic Pressure Transducer. The entire instrument has been calibrated by lifting a series ofweights.

(d) To measure the elongation of the specimen two Daytronic Linear Displacement Transducers (G and H) are used, the cores touching the end face of the dumb-bell shoulders. The readings of the two transducers are added together to give the total net elongation of the specimen.

(e) The signal of the three transducers is measured and printed out on a Hewlett Packard digital voltmeter with scanner and printer. It takes about 2 seconds to scan the three points and over that period the air pressure has been found to be sufficiently constant.

Fig. 7 gives an example of a stress-strain diagram for a graphite dumb-bell obtained with this instrument.

For specimens which fractured during irradiation an estimate was made of the stress at which fracture occurred by glueing the ends together with epoxy resin and determining the fracture stress at room temperature[+]. This supposedly gives an upper limit for the fracture stress during irradiation[++].

The lengths of the different parts of the assembly are measured with a travelling microscope. The accuracy and precision depend largely on the quality of the machining of the specimen and the surface finish. In the most favourable cases the measurements of the dimensions are reproducible to $\pm$ 2µm.

The Young's Modulus of the tensile specimens are measured with the machine described above. The Young's Modulus of all the other parts are measured sonically.

To obtain the rate of unrestrained dimensional changes small control specimens, which have been manufactured from the same material from a point in the block adjacent to that of the specimen, are irradiated together with the creep strain specimens. For the double necked dumb-bells these controls are small split sleeves around the thin neck, their dimensions being sufficiently short in order not to restrain the shrinkage of the neck.

+ This measurement was performed by Mr. J. Meeldijk, Euratom, Petten.

++ The glue was of course always stronger than the graphite.

One half sleeve is made of the dumb-bell material, the other half of the sleeve-material. These control specimens have the additional advantage that they fill up the space which otherwise would contain trapped air, which might damage the specimen by oxidation during the irradiation.

For the single-necked dumb-bells small rods, 3.2 mm in diam., 10-20 mm long serve as controls.

The compressive specimen is surrounded by a spacer which gives the unrestrained dimensional changes.

In cases where these specific controls are lacking, for instance for the inner and outer restrainer in the compressive assembly, use is made of data on normal specimens in the same capsule or of data available for comparable specimens from previous irradiations.

It was also found that the dimensional changes of the dumb-bell shoulders give a reasonable indication of the free shrinkage of the dumb-bell material.

The irradiations were carried out in the core of the High Flux Reactor (H.F.R.) at Petten, The Netherlands. The H.F.R. is an enriched uranium fuelled, light water moderated and cooled, materials testing reactor. Initially the irradiations were performed in position E7, and later, when the reactor power was increased from 20 to 30 MW, in E8. Both were positions at the edge of the core. More recently, when the need was felt to enhance the damage rate, (to speed up the experiments) the capsule was transferred to position C5 in the centre of the core where the neutron flux density is approximately 70% higher than in the edge position.

A fully instrumented irradiation capsule was used with three temperature regions, controlled at 600°C, 900°C and 1200°C respectively. Recently the capsule design was modified and a fourth temperature region, at 800°C, was included.

The capsule consisted of graphite drums as specimen carriers, surrounded by a stainless steel can. Each drum was equipped with a separate electrical resistance heater to supplement and to compensate for variations in the γ-heating. The gas in the capsule was clean helium at a pressure of 4 atm. The capsule was thoroughly degassed prior to irradiation to avoid corrosion of specimens and heaters.

Ten capsules have been irradiated so far with irradiation times per capsule up to seven reactor cycles (a reactor cycle is about 18 days). In most capsules a fairly accurate temperature control was reached during the irradiation. In the 600°C drum the temperature gradient was generally less than 50°C and the temperatures remained constant during the entire irradiation

to within ± 15°C. In one case (due to heater failure) the temperature dropped to 500°C and roseslowly to 600°C in the course of a reactor cycle. Unless stated otherwise the specimens in the 600°C drum are considered to have been irradiated at 600°C± 30°C. In the 900°C drum, situated at the peak of the γ-flux distribution curve, a very constant temperature and a small thermal gradient, of the order of ± 30°C, was obtained. So the specimens in the 900°C drum are considered to have been irradiated at 900°C± 30°C. There was a rather pronounced thermal gradient over the 1200°C drum, with temperatures ranging from 1100°C-1250°C, but in most cases the temperatures were well defined and sufficiently constant (±15°C).

The neutron flux distribution in the capsule had its peak at the position of the 900°C drum. In that drum the fast flux, determined by nickel activation, ranged from 0.9 to 1.1 x 10^{14} n.cm^{-2}s^{-1} in the edge-of-core position and is around 1.7 x 10^{14} n.cm^{-2}s^{-1} in the present mid-core position. For both the 600°C and 1200°C drums these average fast flux densities are 0.6 x 10^{14}n.cm^{-2}s^{-1} and 1.1 x 10^{14} n.cm^{-2}s^{-1} for the edge-of-core and mid-core position respectively.

The neutron exposures were measured by activation of nickel, iron and cobalt, making use of the activation reactions Ni-58(n,p) Co-58 and Fe-54(n.p)Mn-54, for the calculation of the fast flux and Co-59(n,γ)Co-60 and Fe-58(n,γ)Fe-59 for the thermal flux. The values of the integrated fast flux used throughout this paper are given in terms of an equivalent integrated fission flux. For comparison of results with those obtained in other reactors use can be made of the conversion factors given in table I (Ref. D.L. Reed et al. [9]).

4. ACCURACY

The main sources of uncertainty are presently both the stress measurement and the measurement of the strain rate. The tensile test may be considered rather reliable at the low strains encountered. The values obtained for the Young's Modulus are generally up to 10% lower than those obtained with a sonic test on normal rod specimens after irradiation under identical conditions (except for the stress). The reproducibility is generally better than 5%.

It is the thermal expansion measurement that is the largest source of error here. Characteristically the total elongation is of the order of 100 μm for specimens at 600°C and 200 μm for specimens at 900°C and 1200°C. The reproducibility varies from ± 0.2 μm to ± 5.0μm and it is not clear why it is so different for different specimens. Since the elastic elongation is

of the order of 10 - 30μm it can be seen that the errors may be large in the worst cases and in the best cases they are several per cent.

The second source of uncertainty lies in the knowledge of the free dimensional changes. This is in part due to the fact that the radiation creep strain in this kind of experiment is the difference of dimensional changes shown and those not shown (but expected). This last figure must be obtained from different specimens and it is well known that there may be an appreciable scatter in the properties and behaviour even with specimens which are cut out adjacently. This point is well illustrated for the restrainer material in figure 8.

As an example, the free shrinkage rate of a certain dumb-bell material between 3 and 6 x 10^{20} $n.cm^{-2}$ was found to be in between -0.13% and -0.08% per 10^{20} $n.cm^{-2}$, Likewise the expansion rate of the sleeve lies in the range +0.04% and +0.05% per 10^{20} $n.cm^{-2}$ so the rate of differential shrinkage, which determines the stress for a given creep constant, might be as high as 0.18% per 10^{20} $n.cm^{-2}$ and as low as 0.12% per 10^{20} $n.cm^{-2}$. This may possibly be a rather extreme example, but it is clear that this factor directly influences the creep constant obtained. Taking all these factors together it may be stated that in most cases the results for tensile creep are accurate $\pm$ 20%.

For the compressive creep the accuracy is somewhat lower both for results on compressive assemblies and on the restrainer in the tensile assemblies. In the former case the dimensional behaviour of the outer restrainer shows relatively large scatter and it is rather uncertain how effects of the threaded plug must be taken into account. Furthermore any change in position of the plug, for instance due to vibration, alters the stress.

In the latter case the stress levels are usually extremely low and consequently the steady state creep strain is small relative to the scatter in the dimensional changes and the apparent strain due to a change in thermal expansion.

5. MATERIALS

A number of different graphites obtained from all the major European Manufacturers was used in the present experiment. The different graphites have been indicated by a Reference Number (Ref. no.) throughout this paper. These are not to be confused with the Bibliographic references which are indicated by a number in square brackets | | .

A brief description of the various materials is given below.

Ref.no.			
2	pressed	coarse grain	low thermal expansion well developed crystallinity
6	extruded	Ford's pitch coke	isotropic
7	extruded	particle agglomeration	isotropic
16	extruded	Gilsocarbon	high thermal expansion
21	extruded	Gilsocarbon	isotropic, high thermal expansion
22	hot pressed		highly anisotropic well developed crystallinity
35	pressed	fine grain	high strength, anisotropic
61	extruded	very fine grain + ∿30% carbon black	anisotropic, high Young's Mod.
71	extruded	Gilsocarbon	high thermal expansion
95 } 595	pressed	Gilsocarbon Triply impregnated	isotropic
105	isostatically pressed	resin bonded natural graphite	

Of these Ref.no. 61 is an extremely fast shrinking graphite and use has been made of this material as outer restrainer for the compressive assemblies. Ref.no. 22 expands in the direction parallel to the pressing direction as shown in figure 8. This material was mainly used for the restraining split sleeves in the tensile experiment.

6. RESULTS

The dimensional changes observed in the components of a typical assembly together with those of unstressed specimens are illustrated by Fig. 9.

The progressive increase in stress with increasing effective irradiation dose of a typical tensile specimen irradiated with restraining sleeves at 900°C is shown in Fig. 10. Also presented in this figure is the stress build-up as calculated for this particular assembly using the free dimensional changes of the components, their Young's Moduli and the Q-value obtained from the experimentally determined stress at the highest neutron fluence available. By integrating over this stress build-up to calculate the transient and steady state creep strain the restrained dimensional changes are obtained. An example is shown in figure 11. The value of the creep constant giving the

best fit with the observed dimensional changes was in this case about 15% larger than that obtained from the stress build-up only.

The results of the determination of the radiation creep constants is given in tables III-VI inclusive for the tensile creep experiment. In tables VII-X inclusive data are given for compression. In tables VII, VIII and IX most of the data were obtained from the restraining sleeves in the tensile experiment at very low compressive stresses. In table X most of the data were obtained from inner restrainers in the compressive assemblies. These data are probably not very accurate since the stress distribution in the inner restrainer is rather inhomogeneous. At higher stress levels an indentationdue to the much thinner specimen is seen in the inner restrainer. Therefore ranges of value are given only for low neutron doses.

In addition to the value of the radiation creep constants the tables also give the neutron fluence, the observed stress, the Young's Modulus and the observed steady state creep strain. Tensile creep strains up to 2% have been observerd. To find the apparent strain due to changes in thermal expansion in some cases the preirradiation value, obtained for the temperature interval 20-400°C, had to be extrapolated to the irradiation temperature.

In many cases the change in thermal expansion coefficient was found to be quite appreciable. Generally a decrease was found for specimens which had been in tension and a rather marked increase for the restraining sleeves (Material Ref.no. 22). As an example for this material the mean coefficient of linear thermal expansion over the temperature interval 20-1230°C was found to have changed from $10.6 \times 10^{-6} deg.C^{-1}$ to values ranging from $12.6\text{-}15.5 \times 10^{-6} deg.C^{-1}$, giving apparent compressive strains up to ∿0.6%. Insufficient data are available for unrestrained specimens to say with certainty that the changes observed are determined by the radiation creep process.

For most cases also the steady state creep strain calculated for the specimen in the manner explained above is given. In view of the simplifying nature of the calculation and the many uncertainties in the data the agreement with the observed data can be regarded satisfactory. The data for tensile creep are summarised in table X and in figure 12, showing the temperature dependence of the radiation creep constant.

7. DISCUSSION

The results as summarized in figure 12 show a rather broad band of radiation creep constants. These results are substantially in agreement with data obtained by other workers, generally with more direct methods.

That the results are of the correct order of magnitude is confirmed by the survival of most specimens and the fracture of some specimens and by the general consistency of observed stresses and restrained dimensional changes.

A number of questions remain:

1° Is the creep constant indeed a constant or does it change with dose and/or stress level? It is seen that only in a few cases the creep constant found after two successive irradiations is equal or nearly so. In most cases however the values can be said to be constant within the estimated accuracy of ± 20%. It is difficult to find out from this kind of experiment whether a stress dependence of the creep constant exists. It is an essential point of this type of experiment that in materials with a high creep constant a low stress is developed so unless one uses different restraining materials with differing dimensional change with one specimen material to obtain different restraining rates this problem cannot be settled.

In principle the data for Ref.no. 22 under compression could give an indication of this sort. Indeed the values of the creep constant obtained at high stresses are the lowest values found but also at low stresses sometimes low values are obtained. Moreover at very low stresses values tend to become unreliable, and in general the scatter in values is quite appreciable. Finally Ref.no. 22 is a rather unusual material (hot pressed). The same considerations hold for the results in compression for Ref.no. 16.

2° Are radiation creep constants equal for tension and compression? The only materials for which data are available are Ref.no's 16 and 95. Within the experimental accuracy the radiation creep constants for compression and tension are equal here. It should be mentioned that both materials are isotropic, Gilsocarbon based materials and the behaviour of anisotropic reactor graphite based on different filler materials could well be different.

3° Is a creep constant specific for a material? In general there were insufficient duplicate specimens to answer this question with certainty. In general specimens from the same material, cut in the same direction or made from isotropic material, gave creep constants lying rather close together. Examples are Ref.no's 21 and 95. As already mentioned Ref.no. 22 showed a very wide range of values but this is probably due to experimental uncertainties. For this material also the dimensional changes show rather marked scatter, certainly for specimens taken from different blocks.

4° Is the radiation creep constant dependent on the direction in the block? Only in one case, Ref. 35, there was sufficient anisotropy to give a marked difference for two directions in the material. In this case both at 900°C and 1200°C the tensile radiation creep coefficient was larger for the direction parallel to the pressing direction. This could be due to other effects however (see 5°).

5° Is there a correlation between the radiation creep constant and other physical properties? This is not quite clear. By looking at the tables it appears that at 600°C and 900°C specimens with the lowest Young's Modulus have the highest radiation creep constants (for example Ref.no. 35 axial). Although this material has a high creep constant at 1200°C also, certainly at 1200°C there is no very clear indication that such a correlation does exist.

6° No indication was obtained about the existence of a creep strain limit. In practically all cases fracture of a dumb-bell was found to be due to overstressing caused by a too high strain rate.

Summarizing these points it appears that the experiment has yielded values for the radiation creep constant sufficiently well defined to be of technological importance for the design of High Temperature Gas Cooled Reactors. The data are as yet insufficient to state with certainty that different materials behave differently under stress when irradiated. Neither is it possible to correlate the creep behaviour with other measurable properties.

8. CONCLUSIONS

1° The radiation creep constants found lie in the range $2 - 8 \times 10^{-12}$ $(\text{dyne.cm}^{-2})^{-1}$. $(10^{20}\ \text{n.cm}^{-2}\ \text{Ni DIDO})^{-1}$ at 600°C, $4 - 11 \times 10^{-12}$ $(\text{dyne.cm}^{-2})^{-1}$ $(10^{20}\ \text{n.cm}^{-2}\ \text{Ni DIDO})^{-1}$ at 900°C and $5 - 25 \times 10^{-12}$ $(\text{dyne.cm}^{-2})^{-1}$ $(10^{20}\ \text{n.cm}^{-2}\ \text{Ni DIDO})^{-1}$ at around 1200°C. Most specimens showed values at the lower end of these ranges.

2° The radiation creep constant increases with temperature in the range 600 - 1200°C.

3° The behaviour of many different graphites was found to be rather similar. Within the experimental limitation no significant difference between creep in tension and in compression was observed. No correlation with other material properties could be firmly established.

4° The restrained shrinkage experiment, expecially with the post-irradiation examination and the analysis of the results described here, can be very useful for the determination of the radiation creep constant of graphite.

It is shown that the results agree very well with those obtained with more complicated methods.

The main advantages of the method are

1. the small specimen size and therefore comparatively low irradiation cost
2. extreme simplicity of the parts to be irradiated.

Its main limitation is in the accuracy.

The uncertainty is estimated to be $\pm$ 20%. This is mainly due to the post-irradiation measurements, some parts of which are very critical

9. APPENDIX

The derivation of the stress build-up formulae.

The symbols used in this part are listed on the next page.

Ideally, at the beginning of the irradiation the parts A, B and C are just making contact so that N (effective) equals D (total). In practice some of the experiments are so designed that at the beginning of irradiation at the irradiation temperature there is already some initial stress.

At the beginning of irradiation at irradiation temperature:

$$L_A(0) + L_B(0) = L_C(0) \qquad (1)$$

At the end of the irradiation to a neutron fluence N_1 at irradiation temperature the lengths of the three components under stress are determined by:

(a) irradiation induced dimensional changes, generally

$$\frac{\Delta L}{L_o} = a_1 N_1^2 + a_2 N_1 + a_3 \text{ [x]} \quad \text{etc.,}$$

(b) steady-state irradiation creep strain, ε_{II}

(c) the transient creep strain, ε_I

(d) the elastic strain,

$$L_A(N_1,\sigma)=L_A(0).\left[1+a_1N_1^2+a_2N_1+a_3+k_A\int_o^{N_1}\sigma_A(N)dN+\frac{\sigma_A}{E_A}(1-e^{-aN_1})+\frac{\sigma_A}{E_A}\right] \qquad (2A)$$

$$L_B(N_1,\sigma)=L_B(0).\left[1+b_1N_1^2+b_2N+b_3+k_B\int_o^{N_1}\sigma_B(N)dN+\frac{\sigma_B}{E_B}(1-e^{-aN_1})+\frac{\sigma_B}{E_B}\right] \qquad (2B)$$

$$L_C(N_1,\sigma)+L_C(0).\left[1+c_1N_1^2+c_2N+c_3+k_C\int_o^{N_1}\sigma_C(N)dN+\frac{\sigma_C}{E_C}(1-e^{-aN_1})+\frac{\sigma_C}{E_C}\right] \qquad (2C)$$

At the end of the irradiation at irradiation temperature:

$$L_A(N_1,\sigma) + L_B(N_1,\sigma) = L_C(N_1,\sigma) \qquad (3)$$

[x] a_3, b_3 and c_3 should be zero. It was felt however that, in order to account for initial effects, it was more realistic to make a_3 non-zero in some cases.

	A	B	C	Unit
Tensile assembly	Thin neck	Thick neck	Split sleeve	
Compressive assembly	Specimen	Inner restrainer	Outer restrainer	
Pre-irradiation length	L_A (0)	L_B (0)	L_C (0)	μm
Radiation creep constant	k_A	k_B	k_C	(dyne $cm^{-2} \times 10^{20}$ n cm^{-2})$^{-1}$
Young's Modulus	E_A	E_B	E_C	10^{10} dyne cm^{-2}
Equilibrium stress	σ_A	σ_B	σ_C	dyne cm^{-2}
Length as a function of irradiation, shrinkage and creep, under stress, at irradiation temperature.	$L_A(N,\sigma)$	$L_B(N,\sigma)$	$L_C(N,\sigma)$	μm
Neutron fluence effective for creep	N	N	N	10^{20} n cm^{-2}
Total neutron fluence	D	D	D	
Cross sections	O_A	O_B	O_C	cm^2
A tensile stress is taken as positive, a compressive stress as negative.				

σ_A, σ_B and σ_C are related to each other in the following way:

$$\sigma_B = \frac{O_A}{O_B}\,\sigma_A = f_B\,\sigma_A \qquad (4A)$$

$$\sigma_C = -\frac{O_A}{O_C}\,\sigma_A = -f_C\sigma_A$$

from equations (1), (2), (3) and (4) it follows:

$$\sigma_A\{1+(1-e^{-aN_1})\} = -\frac{L_A(0)a_1+L_B(0)b_1-L_C(0)c_1}{\bar{L}}\,E_A.N_1^2-$$

$$-\frac{L_A(0)a_2+L_B(0)b_2-L_C(0)c_2}{\bar{L}}E_AN_1-\frac{L_A(0)a_3+L_B(0)b_3-L_C(0)c_3}{\bar{L}}.E_A-$$

$$-\frac{k_AL_A(0)+k_Bf_BL_B(0)+k_Cf_CL_C(0)}{\bar{L}}.E_A\int_0^{N_1}\sigma_A(N)dN \qquad (5)$$

where $\bar{L} = L_A(0) + f_BL_B(0)\,\frac{E_A}{E_B} + f_CL_C(0)\,\frac{E_A}{E_C}$

This can be written as

$$\sigma_A(N)\{1+(1-e^{-aN})\} = R_1N^2 + R_2N + R_3 - Q\int\sigma_A(N)dN \qquad (6)$$

where $R_1 = -\frac{L_A(0)a_1 + L_B(0)b_1 - L_C(0)c_1}{\bar{L}}.\,E_A$ (6a)

$$R_2 = -\frac{L_A(0)a_2 + L_B(0)b_2 - L_C(0)c_2}{\bar{L}}.\,E_A \qquad (6b)$$

$$R_3 = -\frac{L_A(0)a_3 + L_B(0)b_3 - L_C(0)c_3}{\bar{L}}.\,E_A \qquad (6c)$$

$$Q = k^+.E_A = \frac{k_AL_A(0) + k_Bf_BLB(0) + k_Cf_CL_C(0)}{\bar{L}}.\,E_A \qquad (6d)$$

It can be seen that R_1 and R_2 are effective stressing rates for the assembly.

k^+ is the effective radiation creep constant for the assembly as a whole.

Equation (6) has the following boundary condition:

$\sigma_A = \sigma_o$ for N=0

The solution of equation (6) is:

$$\sigma_1(N) = e^{-\int \frac{F_2(N)}{F_1(N)}\,dN} \int \frac{F_3(N)}{F_1(N)}\, e^{\int \frac{F_2(N)}{F_1(N)}\,dN}\, dN + \sigma_o e^{-\int \frac{F_2(N)}{F_1(N)}\,dN} \qquad 7$$

where $F_1(N) = (2-e^{-aN})$ 8

$F_2(N) = (k^+.E_A + ae^{-aN})$ 9

$F_3(N) = (2R_1N+R_2)$ 10

$$\int \frac{F_2(N)}{F_1(N)}\,dN = \frac{k^+.E_A+2a}{2a} \ln (2-e^{-aN}) + \frac{k^+.E_A}{2}N = \phi(N) \qquad 11$$

$$\sigma(N) = e^{-\phi(N)} \int \frac{R_2+2R_1N}{2-e^{-aN}}.e^{\phi(N)}\,dN + \sigma_o.e^{-\phi(N)} \qquad 12$$

If the beginning of the creep process does not coincide with the beginning of the irradiation, $N \neq D$. Assuming the creep process begins after a neutron fluence D_1. The dimensional changes start at $D = 0$

$$\text{so } N = D - D_1 \qquad 13$$

In that case $L_A(0)$ must be replaced by $L_A(D_1)$ etc.
The formula for the stress as a function of the neutron fluence remains the same, only R_2 has a different value, R'_2.

$$R'_2 = -\frac{L_A(0)\ (2a_1D_1+a_2)+L_B(0)\ (2b_1D_1+b_2)-L_C(0)\ (2c_1D_1+c_2)}{\bar{L}}\ E_A$$

$$= R_2 + 2D_1R_1 \qquad 14$$

The dimensional changes after a total neutron fluence D_2 are

$$\frac{\Delta L_A}{L_A(0)}(D_2) = a_1 D_2^2 + a_2 D_2 + a_3 + k_A \int_{D_1}^{D_2} \sigma_A \, dD + \frac{\sigma_A}{E_A}(1 - e^{-a(D_2 - D_1)}) \qquad 15$$

with the condition $\sigma_A = 0$ for $D_2 < D_1$

10. REFERENCES

1. Perks A.J. and Simmons J.H.W.,
   Carbon 1 441 (1964)

2. Gray B.S., Brocklehurst J.E., Mc. Farlane A.A.,
   Carbon 5 173 (1967)

3. Kennedy C.R., ORNL 3470, p.132 (1963),
   3523 (1963) 227

4. Losty H.H.W., Fielder N.C., Bell I.P., Jenkins G.M.,
   Proc. 5th Conf. Carbon 1961 vol I p. 226

5. Hesketh R.V., Phil. Mag. 11 929 (1965)

6. Perks A.J. and Simmons J.H.W.
   Carbon 4 85 (1966)

7. Jackson J.L., Hart W.E.,
   Carbon 3 94 (1965)

8. Everett M.R., Blackstone R., Graham L.W. and Manzel R.
   Dimensional and Physical Changes of High Temperature Reactor
   Graphite Irradiated at Temperatures in the Range 600-1200^{o}C.
   Presented at the IXth Carbon Conference, Boston, June 1969
   to be published in Carbon.

9. Reed D.L., Everett M.R., and Blackstone R.,
   The correlation of Graphite Irradiations in the High Flux
   Reactor Petten and in High Temperature Reactors,
   I.A.E.A. Symposium Radiation Damage in Reactor Materials,
   paper E7, Vienna, June 1969

10. Henson R.W., Perks A.J., and Simmons J.H.W.,
    Lattice parameter and dimensional changes in
    graphite irradiated between 300 and 1350^{o}C
    Carbon 6 789 (1968)

Table I. Graphite Damage Correlation Factors.

Facility	Neutron exposure expressed as	To obtain DIDO equivalent (Ni) multiply by
H.F.R.	Equivalent fission fluence	1.0
Dragon	"	1.7
DIDO , PLUTO	"	1.0
GETR / ETR	nvt (E>0.18 MeV)	0.66
Dounreay Fast Reactor[x]	total dose	0.46

[x] Direct comparison with results from D.F.R. should be made with extreme caution. Complications may arise from the difference in flux level with that of other facilities, see Henson et al. |10|

Table II. Some typical properties of the Materials used in the Creep Experiments.

Material Ref.no.	Extruded (E) or Pressed (P)	Density $g.cm^{-3}$	Young's Modulus 10^{10} dyne.cm^{-2}		Electrical Resistivity 10^{-3} ohm.cm		Mean Coefficient (20-400°C) of Thermal Expansion 10^{-6} deg C^{-1}	
			R	A	R	A	R	A
2	P	1.66	9.2	7.0	0.60	0.72	2.0	2.8
6	E	1.67	7.1	7.1	1.98	1.89	5.5	4.8
7	E	1.85	11.0	11.9	0.85	0.78	4.6	4.1
16	E	1.80	8.7	9.6	0.87	0.74	4.5	4.0
21	E	1.74	10.1	10.4	0.95	0.93	5.3	5.3
22	P	1.96	10.5	3.1	0.47	1.85	0.5	10.7
35	P	1.69	8.9	5.6	1.11	1.39	3.0	4.5
61	E	1.79	8.3	16.5	3.70	1.90	4.6	1.9
71	E	1.67	7.7	9.1	1.08	1.00	4.9	6.3
95	P	1.79	8.3	8.6	1.04	1.05	5.0	5.3
595	P	1.83	12.1	12.0	1.03	1.03	5.1	5.4
105	P	1.70	10.3	7.1	1.39	1.97	2.6	3.5

A = axial with reference to forming direction.

R = radial with reference to forming direction.

Table III. Tensile Creep. Results 600-650°C

Assembly	Material Ref.no.	Neutron Fluence 10^{20} n.cm^{-2}	E - modulus 10^{10} dyne.cm^{-2}	Stress 10^{8} dyne.cm^{-2}	Radiation Creep Constant k 10^{-12}(dyne.cm^{-2})$^{-1}$ (10^{20} dyne.cm^{-2})$^{-1}$	Steady State Creep Strain % Calculated	Observed
A2	21 A	8.0	18.8	0.84	2.2	0.18	0.17
		14.5	17.7	1.49	2.5	0.38	0.33
		21.3	15.5	1.53	2.5	0.65	0.70
A3	21 R	10.0	14.1	1.01	2.2	0.26	0.27
		18.3	16.1	0.96	4.3	0.72	0.70
		25.0	13.0	1.41	4.1	1.13	1.27
B2	22(45°)	5.3	6.2	0.43	7.1	0.05	0.05
		10.0	6.2	0.37	8.4	0.15	0.16
C1	2 A	4.4	12.8	0.64	4.0	0.14	0.21
		10.3		2.07 +	5.7	0.29	0.35
C2	6 A	5.9	10.7	0.39	6.9	0.29	0.27
		13.5	10.5	0.94	4.0	0.48	0.53
C3	7 A	7.0	16.1	0.73	5.0	0.29	0.31
		16.2	20.2	0.98	2.5	0.44	0.57
1A31	95 A	7.3	11.5	0.47	3.0	0.10	0.09

+ Specimen fractured. Fracture stress of the rest of the dumb-bell at room temperature.

Table IV. Tensile Creep. Results 800-850°C.

Assembly	Material Ref.no.	Neutron Fluence 10^{20} n.cm^{-2}	E-modulus 10^{10} dyne.cm^{-2}	Stress 10^{8} dyne.cm^{-2}	Radiation Creep Constant k 10^{-12} (dyne.cm^{-2})$^{-1}$ (10^{20} n.cm^{-2})$^{-1}$	Steady State Creep Strain % Calculated	Observed
2A13	21 R	13.4	10.5	0.87	6.3	0.73	0.68
2A22	95 A	12.3	11.0	0.81	3.7	0.36	0.28
2A32	95 A	12.9	10.5	1.03	4.3	0.57	0.66
2A41	95 R	13.3	9.6	0.99	4.6	0.61	0.61

Table V. Tensile Creep. Results 900-950°C.

Assembly	Material Ref.no.	Neutron Fluence 10^{20} n.cm^{-2}	E-modulus 10^{10} dyne.cm^{-2}	Stress 10^{8} dyne.cm^{-2}	Radiation Creep Constant k 10^{-12} (dyne.cm^{-2})$^{-1}$ (10^{20} n.cm^{-2})$^{-1}$	Steady State Creep Strain % Calculated	Observed
A4	35 R	7.7	14.2	1.56	3.2	0.46	0.31
		17.2	11.0	1.94	5.8	1.09	1.36
A5	21 A	8.0	12.5	1.06	5.8	0.46	0.35
		18.0	14.5	2.07	9.3	1.70	2.22
A6	21 R	7.8	12.1	0.91	6.4	0.40	0.41
		17.6		3.34+	<14.1 , >5.9	1.44	1.48
B4	35 A	7.7	7.1			0.32	0.20
		19.0	7.1	0.60	11.2	0.80	0.75
C6	71 A	8.7	12.5	1.45	4.3	0.41	0.43
		19.9		2.35+	3.7	1.18	0.73
3A24	105 A	14.1	13.6	0.61	8.2	0.91	0.85
3A25	95 A	12.0	10.4	1.08	7.7	0.68	0.86
3A33	595 A	12.1	12.8	1.13	10.5	1.25	1.11
A-0	61 A	19.9	22.3	1.94	4.7		1.41

+ Specimen fractured. Fracture stress of the rest of the dumb-bell at room temperature.

Table VI. Tensile Creep. Results 1150 - 1250°C

Assembly	Material Ref.no.	Neutron Fluence 10^{20} n.cm^{-2}	E-modulus 10^{10} dyne.cm^{-2}	Stress 10^{8} dyne.cm^{-2}	Radiation Creep Constant k 10^{-12} (dyne.cm^{-2})$^{-1}$ (10^{20} n.cm^{-2})$^{-1}$	Steady State Creep Strain % Calculated	Observed
A8	21 A	6.0	15.2	0.78	14.7	0.34	0.37
		13.3	11.4	1.85	11.6	1.37	1.39
A9	16 A	6.8	15.3	0.80	7.6	0.26	0.30
		12.4	13.8	2.07	6.8	0.96	0.87
A10	35 R	5.8	11.3			0.28	0.43
		14.2		2.28+	10.1	1.60	1.64
B7	35 A	6.1	7.4	0.42	22.5	0.58	0.49
		15.3	7.1	0.91	>15.9	1.64	1.74
B8	21 R	6.2	14.0	0.90	8.0	0.19	0.29
		14.3	10.7	2.04	10.7	1.36	1.48
B10	22(45°)	3.9	14.8	0			
		13.2	3.9	0.10	> 100++		
C9	2 A	6.4	12.0	1.91	3.3	0.34	0.57
		14.4		1.01+	5.2	0.93	0.88
C10	6 A	5.3	8.7	1.42	7.3	0.19	0.29
		12.0		1.50+	8.5	0.93	0.56
C11	7 A	4.7	14.2	0.33	13.5	0.42	0.43
		9.5	11.8	1.60+	13.8	1.12	1.27
4A26	95 A	9.8	9.4	1.96	7.6	0.99	1.17
4A27	95 R	8.1	9.2	1.64	8.9	0.80	1.11
4A34	105 A	9.8	8.0	0.56	25.8	0.80	1.17
2A	61	15.6	19.5	2.44	7.5		1.82

+Specimen fractured. Fracture stress of the rest of the dumb-bell at room temperature.

++Despite a relatively high rate of restraint practically no stress was observed in the specimen.

Table VII. Compressive Creep.

Results 600-650°C for Material Ref. 22 parallel to pressing.

Assembly	Neutron Fluence 10^{20} n.cm^{-2}	Stress 10^{8} dyne.cm^{-2}	Radiation Creep Constant k 10^{-12} (dyne.cm^{-2})$^{-1}$ (10^{20} n.cm^{-2})$^{-1}$	Steady State Creep Strain % Calculated	Observed
A2	8.0	-0.26	9.6	-0.24	-0.23
	14.5	-0.50	9.1	-0.42	-0.31
	21.3	-0.51	6.6	-0.52	-0.57
A3	10.0	-0.34	6.9	-0.25	-0.26
	18.3	-0.32	5.8	-0.30	-0.30
	25.0	-0.43	5.6	-0.48	-0.53
B2	5.3	-0.14	18.3	-0.05	-0.17
	10.0	-0.12	15.0	-0.12	-0.09
C1	4.4	-0.21	18.3	-0.14	-0.29
	10.3	-0.69	18.7	-0.29	-0.38
C2	5.9	-0.13	11.2	-0.15	-0.14
	13.5	-0.31	11.2	-0.38	-0.41
C3	7.0	-0.24	14.4	-0.26	-0.28
	16.2	-0.33	8.1	-0.44	-0.58
1A31	7.3	-0.15	20.0	-0.21	-0.18
CC2 [x]	6.2	-1.95	6.0		-0.73
	13.2	-3.81	4.4		-1.10

[x] Compressive assembly. All other data from restraining sleeve in the tensile experiment.

Table VIII. Compressive Creep.

Results 900-950°C for material Ref. 22 parallel to pressing.

Assembly	Neutron Fluence 10^{20} n.cm^{-2}	Stress 10^{8} dyne.cm^{-2}	Radiation Creep Constant k 10^{-12} (dyne.cm^{-2})$^{-1}$ (10^{20} n.cm^{-2})$^{-1}$	Steady State Creep Strain % Calculated	Observed
A4	7.7	-0.48	9.9	-0.43	-0.29
	17.2	-0.62	8.3	-0.48	-0.59
A5	8.0	-0.33	15.8	-0.38	-0.29
	18.0	-0.67	6.7	-0.29	-0.50
A6	7.8	-0.28	19.7	-0.37	-0.38
	17.6	-1.08	8.3	-0.26	-0.26
B4	7.7		33.6	-0.37	-0.23
	19.0	-0.18	29.4	-0.64	-0.51
C6	8.7	-0.45	12.4	-0.36	-0.38
	19.9	-0.76	12.5	-1.23	-0.74
3A25x	9.3	-0.36	20.2	-0.55	-0.69
3A33	12.1	-0.38	15.7	-0.58	-0.51
CC4[x]	8.8	-4.95	5.2		-1.13
	20.3	-3.04	4.0		-2.39

[x] Compressive assembly. All other data from restraining sleeves in the tensile experiment.

Table IX. Compressive Creep.

Results 1150-1250°C for Material Ref. 22 parallel to pressing.

Assembly	Neutron Fluence 10^{20} n.cm^{-2}	Stress 10^{8} dyne.cm^{-2}	Radiation Creep Constant k 10^{-12}(dyne.cm^{-2})$^{-1}$ (10^{20} n.cm^{-2})$^{-1}$	Steady State Creep Strain % Calculated	Observed
A8	6.0	-0.25	25.1	-0.17	-0.19
	13.3	-0.60	13.2	-0.38	-0.51
A9	6.8	-0.26	20.8	-0.19	-0.22
	12.4	-0.67	7.1	-0.19	-0.25
A10	5.8			-0.21	-0.22
	14.2	-0.74	8.6	-0.40	-0.39
B7	6.1	-0.13	36.0	-0.28	-0.24
	15.3	-0.30	14.6	-0.38	-0.38
B8	6.2	-0.29	18.0	-0.13	-0.20
	14.3	-0.66	10.5	-0.43	-0.39
C9	6.4	-0.62	8.6	-0.28	-0.46
	14.4	-0.32	7.2	-0.16	-0.01
C10	5.3	-0.46	8.6	-0.11	-0.17
	12.0	-0.49	12.0	-0.38	-0.17
C11	4.7	-0.10	48	-0.32	-0.34
	9.5	-0.52	9.5	-0.30	-0.29

Table X. Compressive Creep. Ref. 16 axial and Ref. 95 axial.

Assembly	Temp. °C	Neutron Fluence 10^{20} n.cm^{-2}	Stress 10^{8} dyne.cm^{-2}	Radiation Creep Constant k 10^{-12}(dyne.cm^{-2})$^{-1}$ (10^{20} n.cm^{-2})$^{-1}$ min.	max.	Observed Creep Strain %	Material
C2	600	6.2	-0.49	3.6	7.2	-0.11	Ref. 16
D2	600	6.4	-0.30	3.7	7.4	-0.07	" "
C3	900	8.7	-0.44	6.1	12.2	-0.24	" "
D3	900	8.8	-0.86	4.6	9.2	-0.35	" "
C4	900	8.8	-1.24	3.9	7.8	-0.43	" "
D4	900	8.8	-1.10	4.5	9.0	-0.44	" "
D4*	900	4.1				-0.69	" "
		8.8	-4.47	5.3		-1.40	" "
		20.3	-2.19	5.8		-2.76	" "
C5	1200	6.4	-1.00	5.0	10.0	-0.32	" "
D6	1200	5.3	-0.40	11.8	23.6	-0.25	" "
C5*	1200	3.4				-0.58	" "
		6.4	-4.05	5.6		-1.09	" "
		12.9	-3.42	4.5		-2.26	" "
2A51*	800	13.4	-3.84	3.9	7.8	-2.03	Ref. 95
2A51	800	13.4	-0.96	2.4	4.8	-0.30	" "

* Compressive Assembly : specimen. All other data from inner restrainers.

Table XI. Tensile Creep. Summary of results.

Radiation Creep Constant k 10^{-12}(dyne.cm^{-2})$^{-1}$(10^{20} n.cm^{-2})$^{-1}$ and maximum observed total creep strain ε(%).

Irradiation Temp.	600 - 650°C		800 - 850°C		900 - 950°C		1150 - 1200°C	
Material Ref.no.	k	ε	k	ε	k	ε	k	ε
2 A	4.8±0.8	0.49					5.2±2.0	0.72
6 A	5.5±1.4	0.64					7.9±1.5	0.73
7 A	3.7±1.3	0.62					13.6±1.5	1.45
16 A							7.2±0.8	1.15
21 A	2.4±0.2	0.80			8.6±3.3	2.57	12.6±2.0	2.38
21 R	3.5±1.2	1.38	6.3±1.2	0.78	9.1±2.7	1.84	9.8±1.5	1.82
35 A					11.2±2.0	0.83	22 ±4	1.87
35 R					4.5±1.3	1.54	10.1±2	1.84
61 A					4.5±0.7	1.41	7.5±1.0	
71 A			4.1±0.3	1.12	4.0±0.5	0.88		
95 A	3.0±0.5	0.13	4.0±0.5	0.76	7.7±0.5	0.96	7.6±1.0	1.38
95 R			4.6±0.5	0.72			8.9±1.0	1.29
595 A					10.0±0.5	1.20		
105 A					8.2±0.5	0.89	25.8±3.0	1.24
22 (45°)	7.7±0.7	0.22					>20	0.63

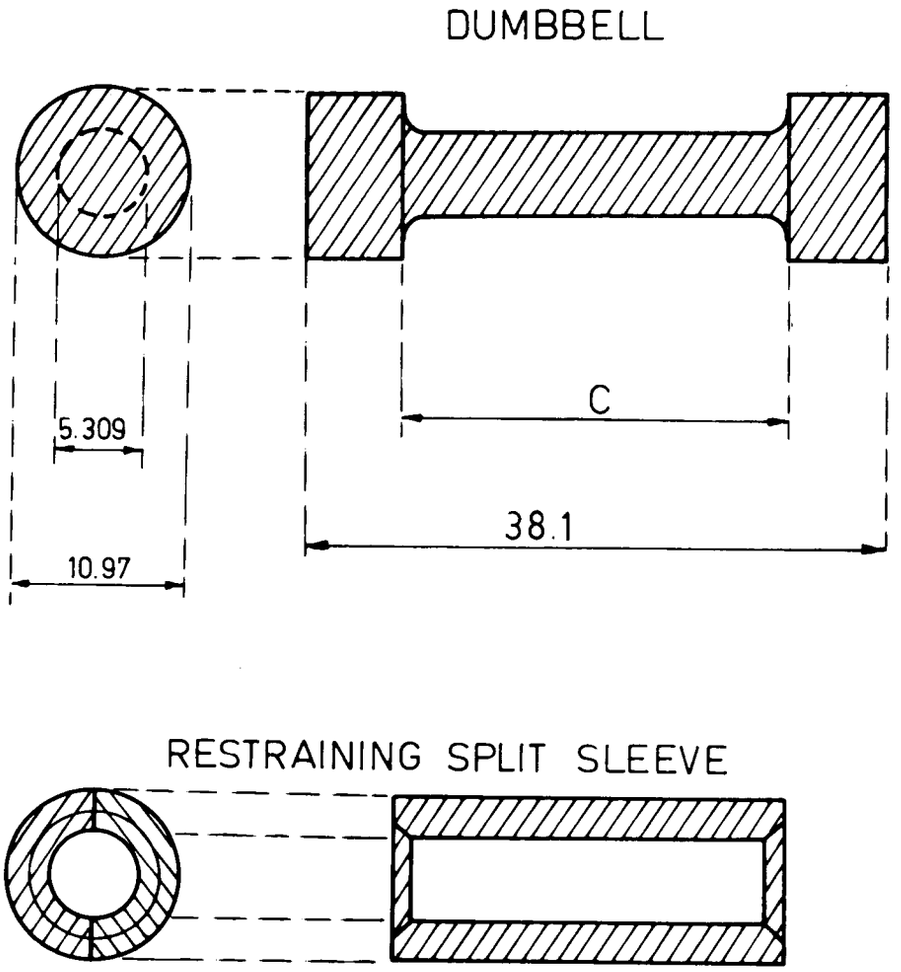

FIG.1 TENSILE CREEP ASSEMBLY SINGLE NECKED

DIMENSIONS IN mm

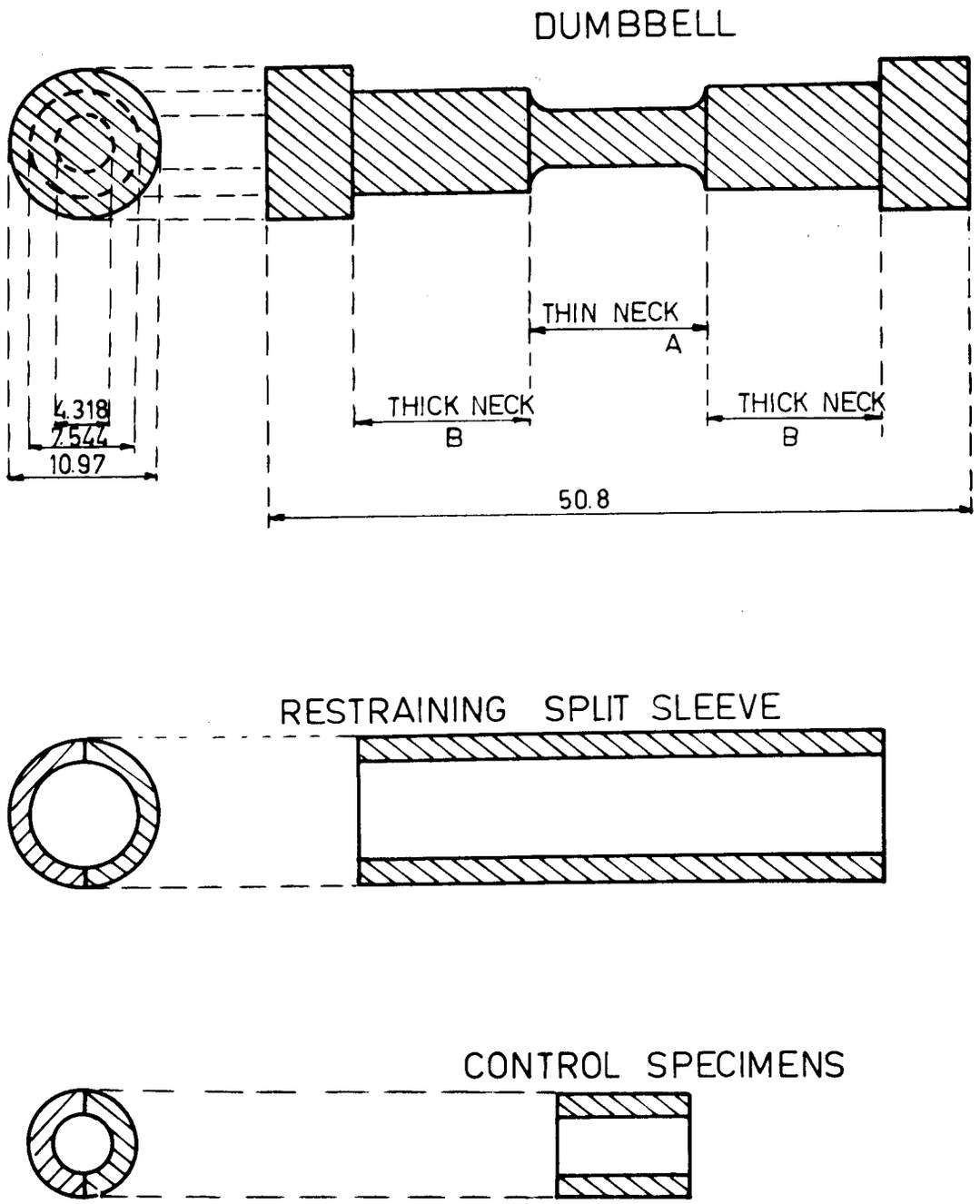

FIG.2 TENSILE CREEP ASSEMBLY DOUBLE NECKED

DIMENSIONS IN mm

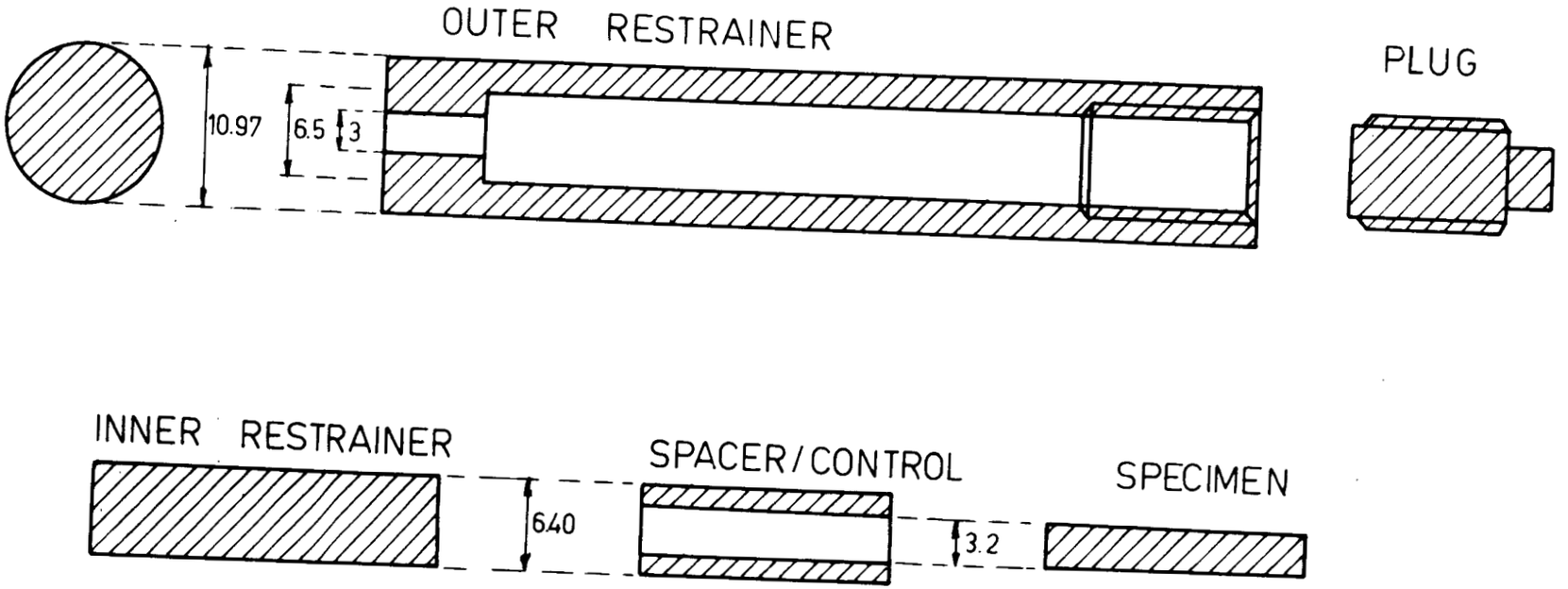

FIG.3 COMPRESSIVE CREEP ASSEMBLY

DIMENSIONS IN mm

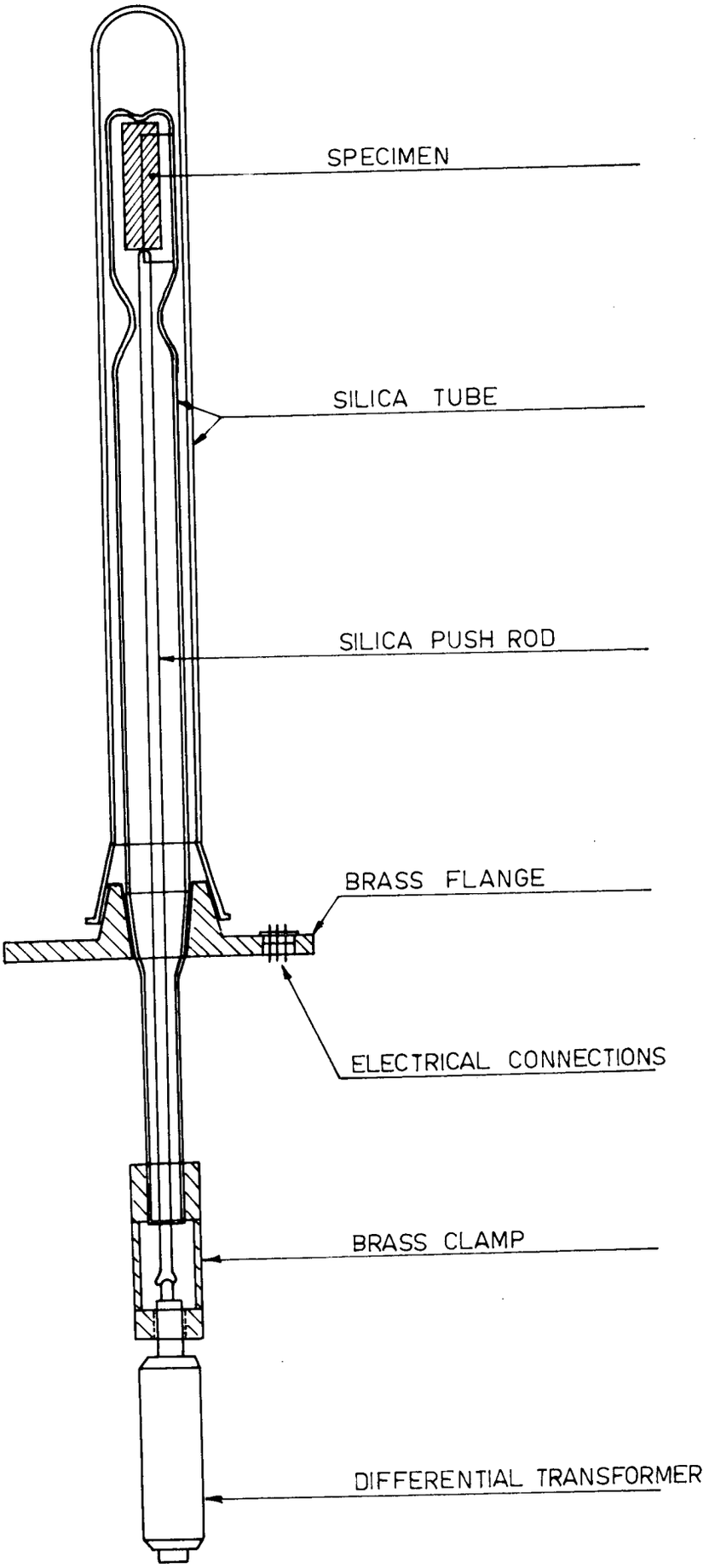

FIG. 4 THE DILATOMETER

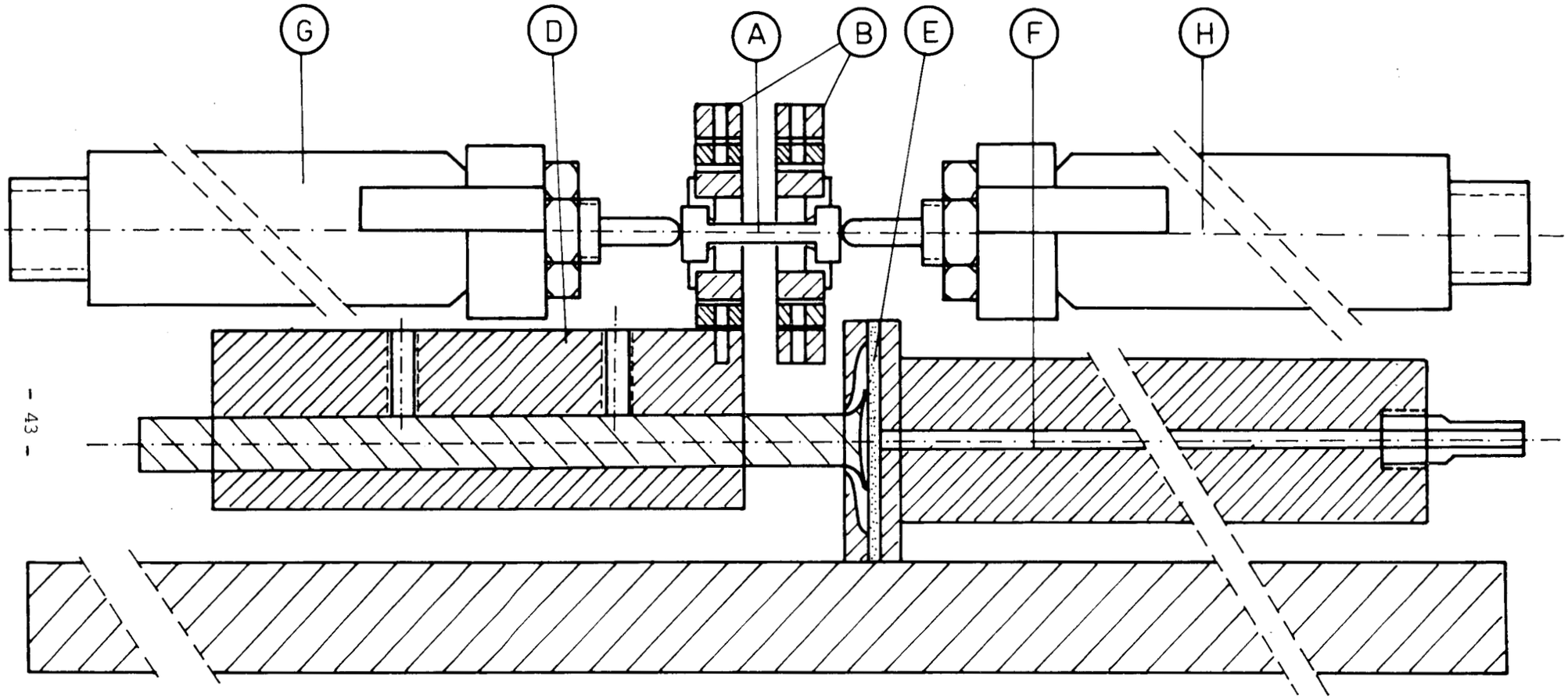

FIG. 5 DIAGRAM OF THE TENSILE TESTING MACHINE

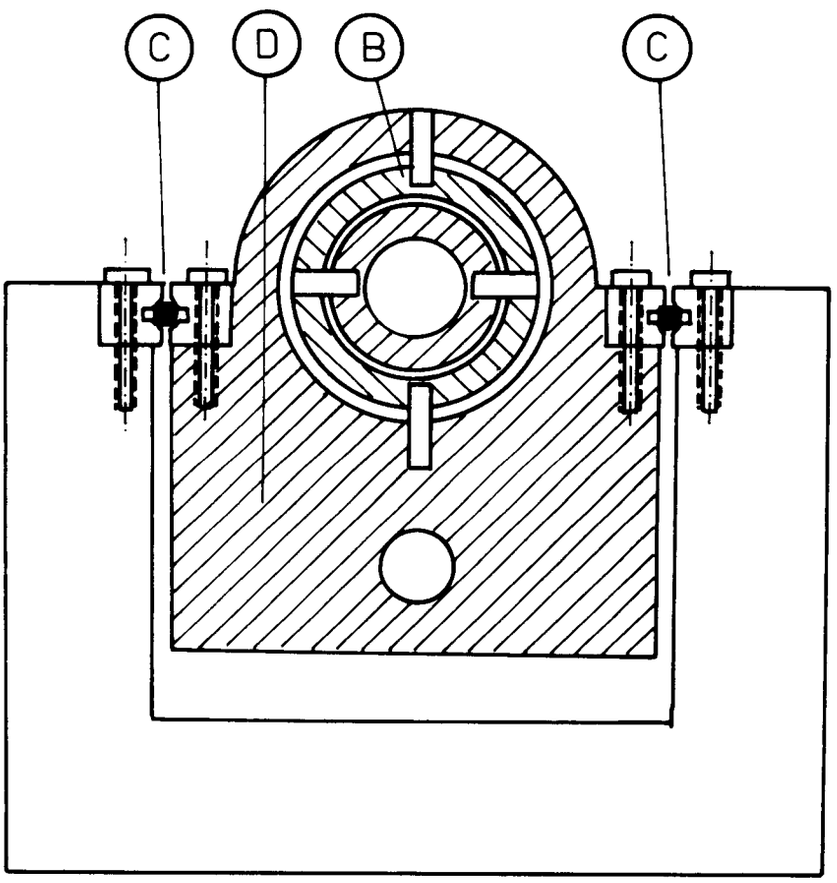

FIG. 6 DIAGRAM OF THE TENSILE TESTING MACHINE

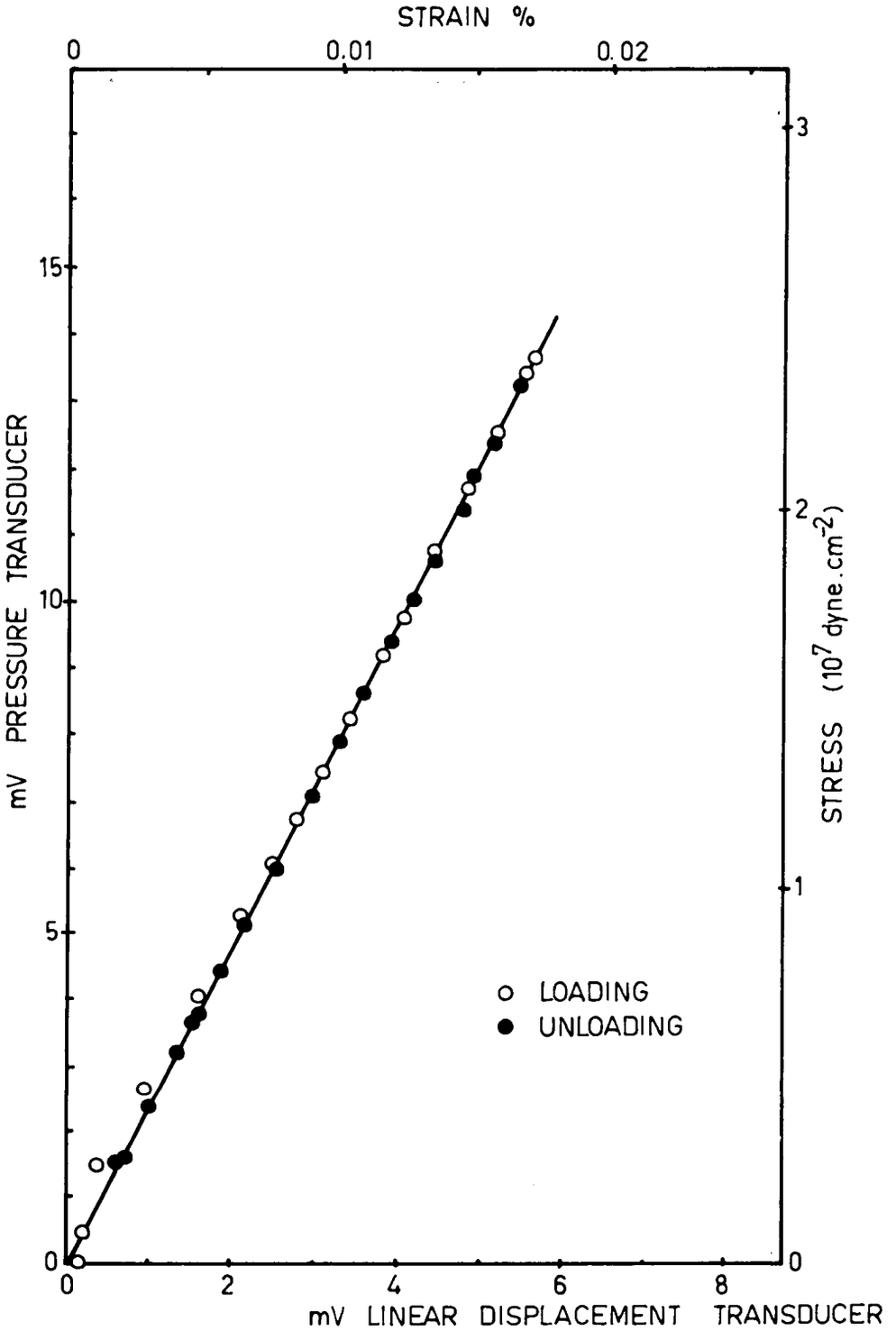

FIG. 7 EXAMPLE OF A STRESS-STRAIN DIAGRAM FOR A SINGLE-NECKED DUMBBELL (Nº B8 REF. 21 L 1200 °C IRR. TEMP.)

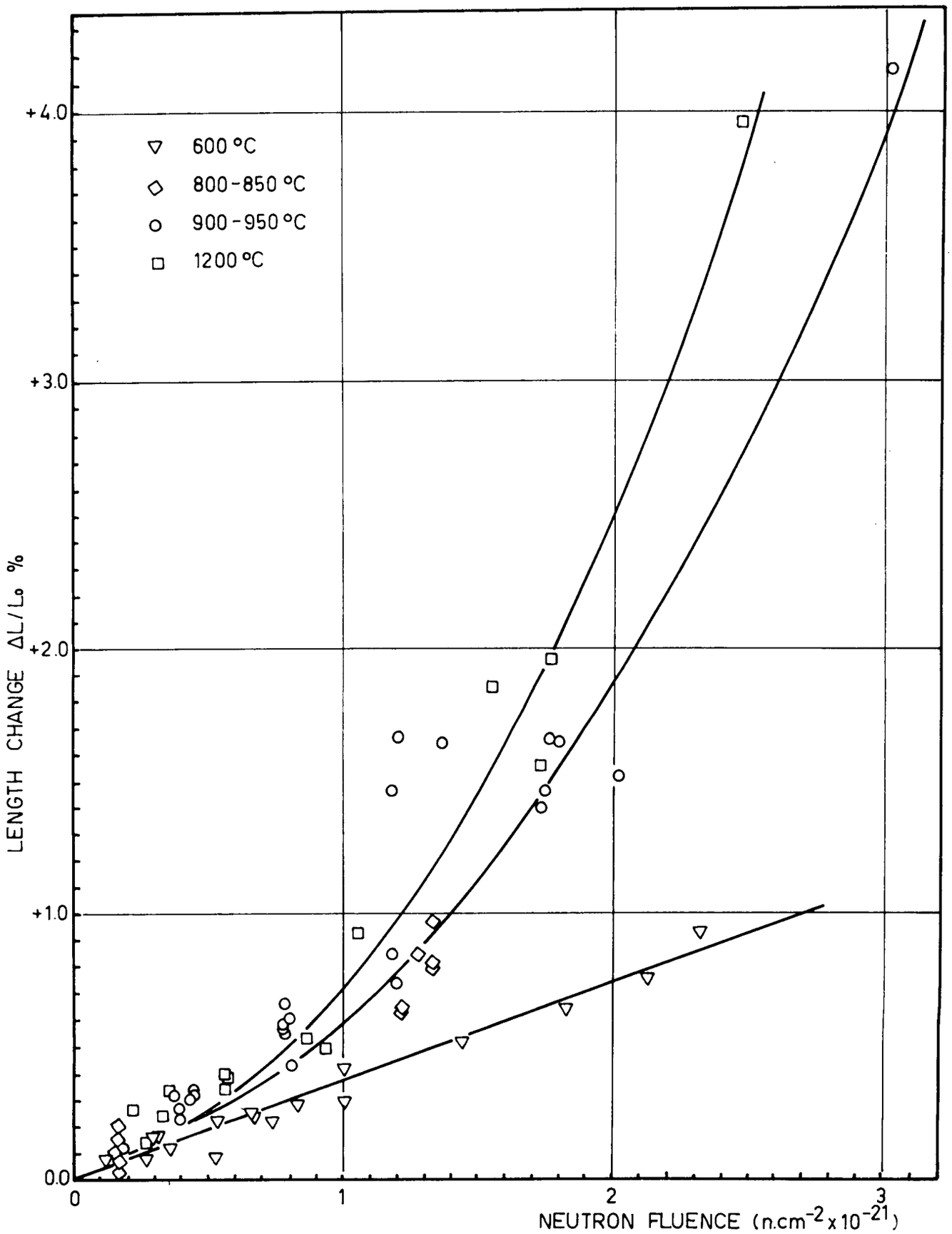

FIG. 8 DIMENSIONAL CHANGES OF GRAPHITE REF. 22 PARALLEL TO PRESSING

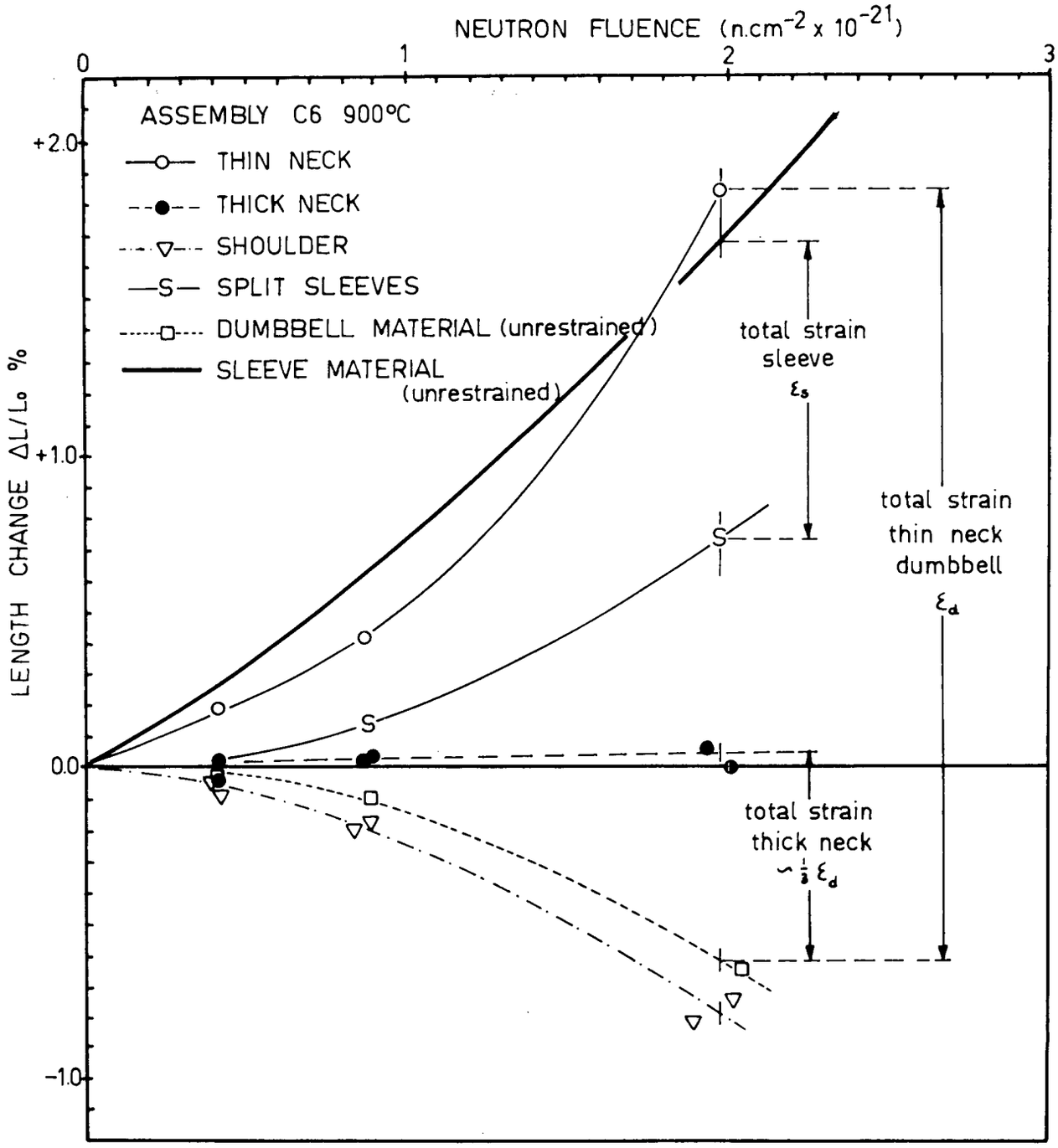

FIG. 9 DIMENSIONAL CHANGES OF THE COMPONENTS OF A TYPICAL TENSILE ASSEMBLY

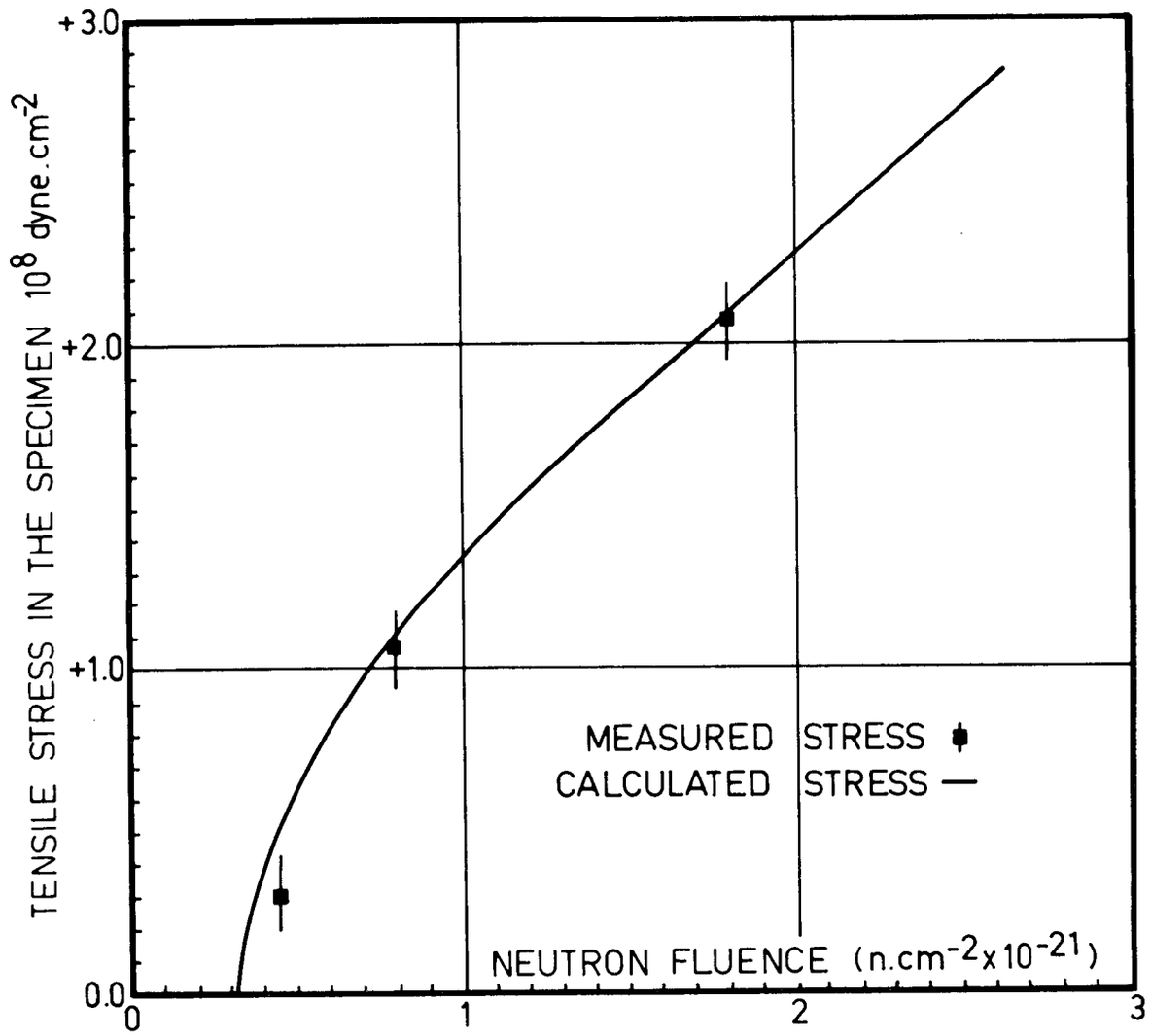

FIG.10 RESTRAINED SHRINKAGE EXPERIMENT. EXAMPLE OF RESULTS AT 900 °C FOR A SPECIMEN OF EXTRUDED GILSOCARBON GRAPHITE REF. 21

STRESS BUILD-UP WITH NEUTRON DOSE.

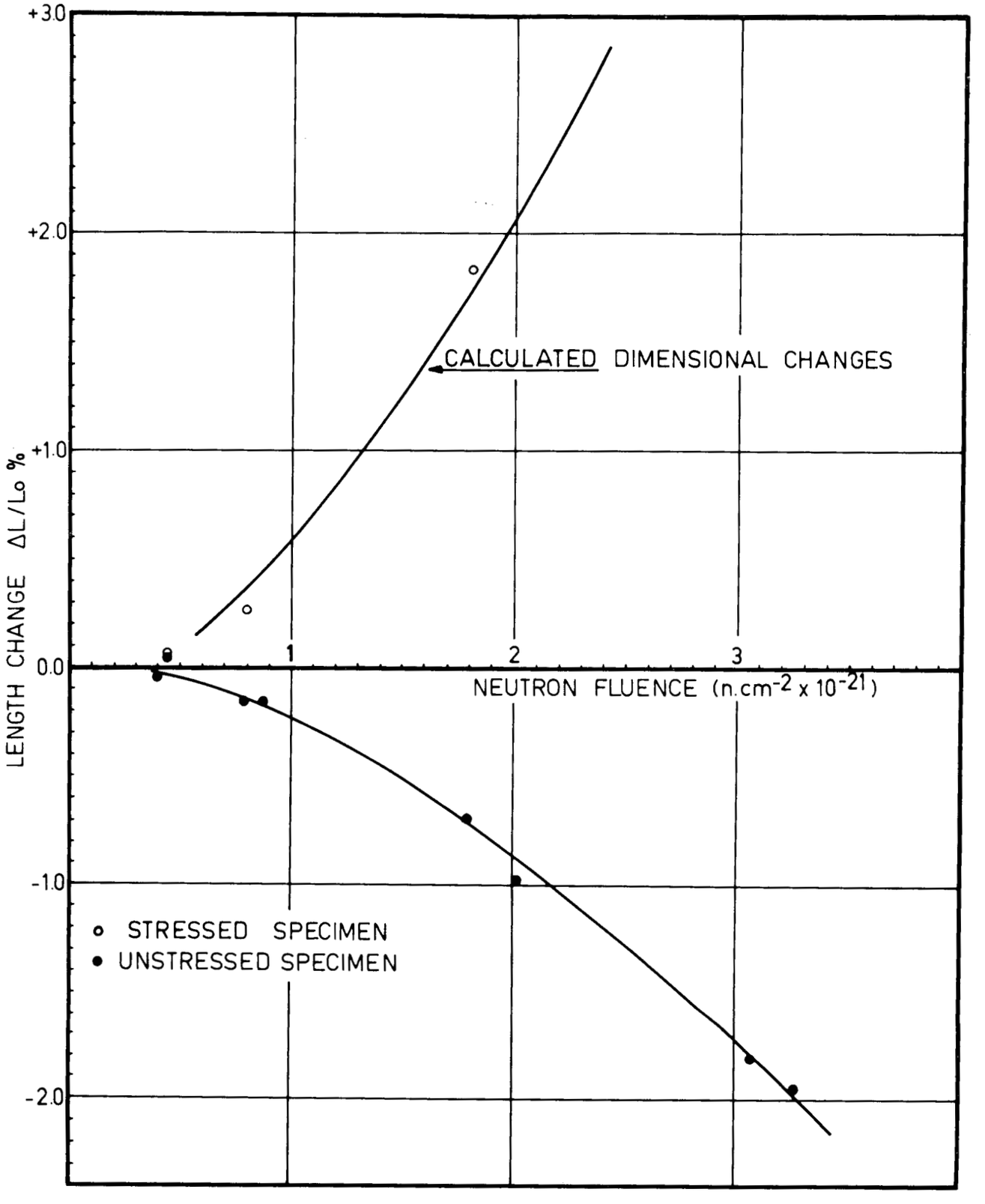

FIG.11 RESTRAINED SHRINKAGE EXPERIMENT. EXAMPLE OF RESULTS AT 900 °C FOR A SPECIMEN OF EXTRUDED GILSOCARBON GRAPHITE REF. 21.

DIMENSIONAL CHANGES OF STRESSED AND UNSTRESSED SPECIMEN. CALCULATED DIMENSIONAL CHANGES FOR STRESS AS GIVEN IN FIG.10 AND DIMENSIONAL CHANGES IN THE UNSTRESSED SPECIMEN, FOR A VALUE OF THE RADIATION CREEP CONSTANT OF 11 $\times 10^{-12}$ $(\text{dyne.cm}^{-2})^{-1}$ $(10^{20}\,\text{n.cm}^{-2})^{-1}$

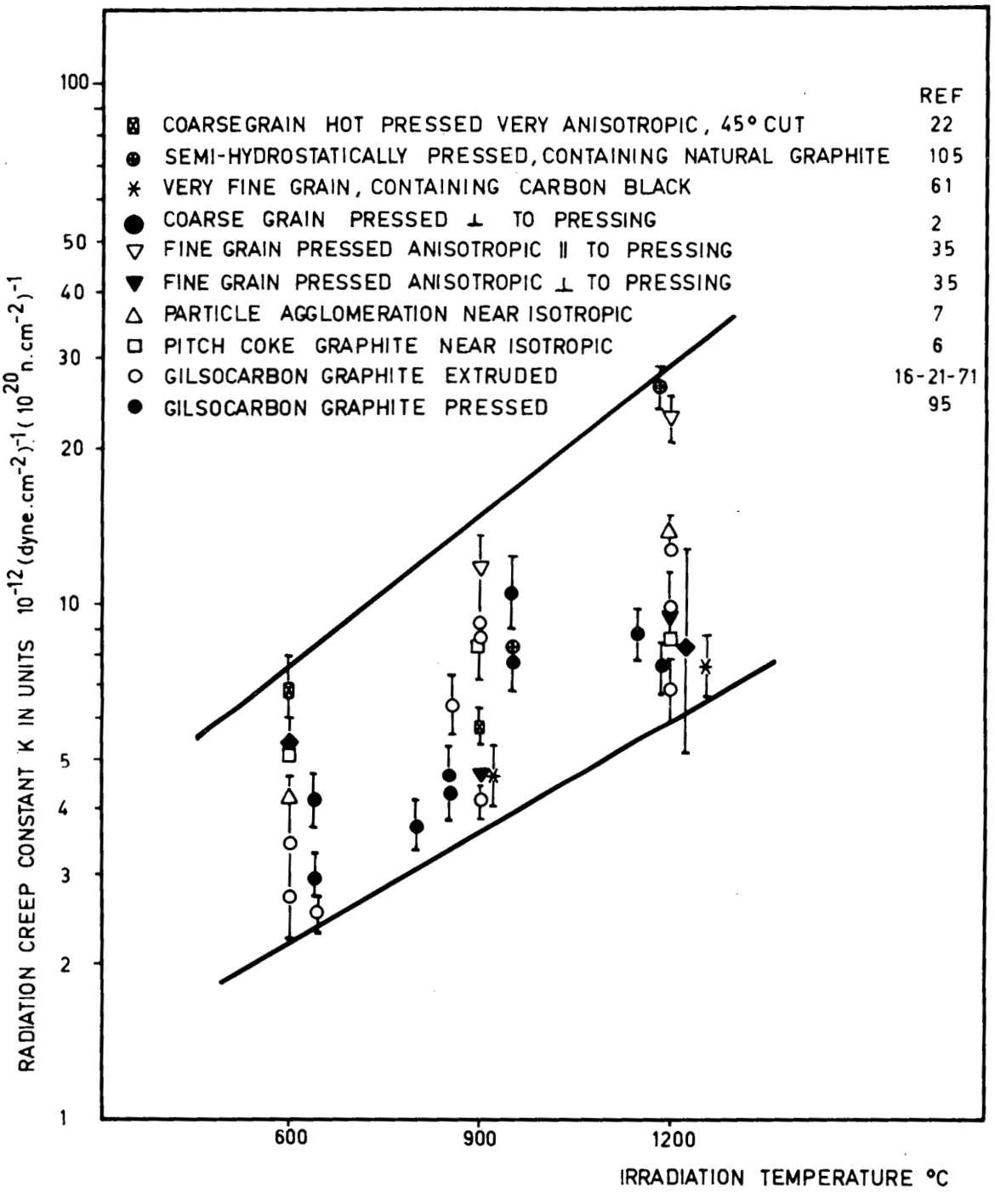

FIG. 12 TENSILE CREEP

THE RADIATION CREEP CONSTANT AS A FUNCTION OF IRRADIATION TEMPERATURE FOR A NUMBER OF DIFFERENT REACTOR GRAPHITES